How to Achieve CDOs for All Aircraft: Automated Separation in TMAs

Enabling Flexible Entry Times and Accounting for Wake Turbulence Categories

Tatiana Polishchuk, Valentin Polishchuk, Christiane Schmidt
Communications and Transport Systems
ITN Department, Linköping University (LiU)
Norrköping, Sweden
firstname.lastname@liu.se

Raúl Sáez, Xavier Prats
Department of Physics - Aerospace division
Technical University of Catalonia (UPC)
Castelldefels, Barcelona, Spain
{xavier.prats, raul.saez.garcia}@upc.edu

Henrik Hardell
Comunications and Transport Systems, ITN Department,
Linköping University (LiU), Norrköping, Sweden
Procedure Design Unit, Luftfartsverket (LFV),
Norrköping, Sweden
firstname.lastname@liu.se

Lucie Smetanová
Comunications and Transport Systems, ITN Department
Linköping University (LiU), Norrköping, Sweden
Czech Technical University, Prague, Czech Republic
{luca.smetanova}@gmail.com

***Abstract*—This work presents an enhanced optimization framework for fully automated scheduling of energy-efficient continuous-descent arrivals with guaranteed separation in the Terminal Maneuvering Area (TMA). On the example of a real heavy-traffic scenario at Stockholm Arlanda airport, we demonstrate that our approach enables scheduling of all planned arrivals during one hour of operation as continuous descents, by allowing flexible time of arrival to entry points within a range of $\pm$ 5 minutes. This provides significant savings in the time and distance aircraft spend inside the TMA. In addition, we integrate different aircraft wake turbulence categories that enable category-specific separation criteria.**[1]

***Keywords*—Separation; MIP; CDO; Sequencing; Pressure**

I. Introduction

Air transportation has undergone a significant growth over the last decades—and while passenger forecasts, like that of the International Air Transport Association (IATA) [1], will have to be adapted because of the setback of 2020 (see, e.g. [2])—high air traffic volumes are projected also for the future. This is accompanied by a high environmental impact and dramatically increased complexity for air traffic control officers (ATCOs)—effects occurring particularly in terminal maneuvering areas (TMAs), as these are especially affected by congestion and noise. Thus, alleviating the environmental impact and ATCO task load in TMAs by an improved design of arrival and departure procedures—while providing a high runway throughput—becomes crucial.

A budding solution to mitigate the environmental impact by optimal engine-idle descents are continuous descent operations (CDOs) [3]. Eurocontrol [4] states that CDOs "allow aircraft to follow a flexible, optimum flight path that delivers major environmental and economic benefits—reduced fuel burn, gaseous emissions, noise and fuel costs—without any adverse effect on safety".

CDOs are optimized to the operating capability of the aircraft, resulting in different optimum trajectories for aircraft with different characteristics. However, at a strategic level, altitude and speed constraints published in standard terminal arrival route (STAR) charts do not take the particular operating capability of each aircraft into account, thus, limiting the possibility of performing optimum descent trajectories. Moreover, the different optimum trajectories result in decreased vertical and temporal predictability of incoming traffic flows, which leads to an increase of the ATCO workload. Hence, ATCOs increase separation buffers leading to airspace and runway capacity losses that are not desirable in major TMAs, especially during peak hours. That is, ATCOs use instructions such as altitude assignments, speed adjustments and path stretching (i.e., radar vectoring, also called *open-loop* instructions) so as to maintain safe separation between aircraft. These techniques, however, tend to degrade the performance of descent operations, leading to a higher environmental impact. Furthermore, neither the duration of such open-loop vector instructions, nor how the aircraft will re-join its initial route is known by the aircraft crew. As a result, it is impossible for state-of-the art flight management systems (FMS) to predict the remaining distance to go and, therefore, to optimize the trajectory to achieve the most environmentally-friendly descent profile. Consequently, in busy TMAs CDOs hardly take place. Thus, automation tools that support ATCOs in the separation task are essential.

In [5], we presented an optimization framework for computing aircraft arrival routes that guarantee temporal separa-

[1]This research is a part of the ODESTA project supported by the Swedish Transport Administration (Trafikverket) and in-kind participation of LFV.

tion of all aircraft arriving to a TMA within a given time period, incorporating realistic continuous descent operation speed profiles: all aircraft fly according to their optimal neutral CDO speed profiles (i.e., descents with idle thrust and no speed-brakes usage). However, in experiments for Stockholm TMA we could accommodate about 78% of flights performing energy-efficient CDO profiles only for arrivals during one hour with average traffic intensity. This limit was not rooted in computational limits of our optimization framework or servers, but in the input: if aircraft undercut the required uniform temporal separation of two minutes already at the entry point, this yields an infeasible problem, and we filtered out these aircraft. A possible solution would be to impose non-optimal speed profiles on aircraft in these cases. However, then we would forfeit the CDO benefits in terms of reduced fuel burn, gaseous emissions, noise and fuel costs.

In this work, we solve the problem: instead of requiring that an aircraft arrives at its entry point to the TMA at a fixed point in time, we assume that speed profiles along en-route segments can be adapted such that an aircraft's possible arrival time falls within a time window, from which we can pick the actual arrival time (linear holding [6] is one way to achieve the flexibility). This allows us to obtain a high runway throughput, crucial for high air traffic volumes—for Stockholm TMA all aircraft arriving during one of the busiest hours of operation can fly CDOs.

Moreover, in our previous work, we required a uniform temporal separation of consecutive aircraft along the arrival routes (we used 2 minutes in experiments)—independent of the aircraft category of the leading and trailing aircraft. In this work, to establish applicability in real-world scenarios, we account for separation that is determined by the leading and trailing aircraft types at each point of our arrival tree (note that merging arrival routes will yield changes in the leading aircraft for a specific arriving aircraft over time).

II. Related Work

Several authors proposed methods to improve separation and sequencing of aircraft within a TMA. In early works [7], NATS and EUROCOTNROL considered sequencing close to the runway with a re-categorization project aiming to replace the current standard of using only a few aircraft categories, where separation is determined by the category of leading and trailing aircraft, by a per-aircraft-type separation standard. Research and development of terminal spacing tools have been ongoing for several years. Older tools focused on increasing runway throughput using complex models of controller behaviour. For example, in [8], the authors adjusted an aircraft's speed profile and provided a heading correction in order to obtain a fuel-efficient descent and reach the desired arrival time. Balakrishnan and Chandran [9] optimized runway throughput using constrained position shifting, that is, they allowed that aircraft can be moved $\pm k$ places in the FCFS arrival queue. Detailed studies have been made for assessing the impact of new concepts in relation to sequencing [10], [11], [12]. Different dimensions have been considered: flight efficiency, e.g., using distance and time flown; human factors, e.g., using workload and radio communications; and effectiveness, e.g., using achieved spacing in final using simulation data. In [13], the authors proposed a novel approach for understanding and characterization of arrival sequencing and pressure, which relies on the evolution of spacing between aircraft over time. and considers aspects as convergence, speed, and monotony. The authors extended the methodology in [14] with an analysis of spacing and pressure for four European airports—each representing a different type of operation. We apply similar methodology with several modifications to compare our optimal solutions to the real arrival routes.

The scheduling of flights performing neutral CDOs in a TMA has been analyzed in [5], [15], where different methodologies were applied to automatize the sequencing and merging process so that the ATCO taskload is reduced. It was shown that, although the scheduling process becomes more challenging due to the lack of flexibility of the CDOs (i.e., the trajectory can only be controlled by means of the elevator), the safety of the operation can be maintained, while improving the efficiency. Benefits of flying neutral CDOs were assessed in [16], where it was shown that flying neutral CDOs would represent fuel savings of around 5% to 30%.

III. Overview of our Approach

A. Concept of Operations

Suppose several aircraft enter an airport's TMA through several entry points (aiming to land). For each entry point, several paths (with different distance-to-go) are available for the aircraft. The paths from all entry points merge at different points inside the TMA, until they all meet at the metering fix.

Once the aircraft enter the TMA, they start a route negotiation/synchronization process with the ATCO (or ground automated system). The aircraft FMS computes and downlinks to the ATCO a set of finite profiles for different path lengths within the TMA. After receiving all the profiles and analyzing the potential routes for each aircraft, ATCOs (with the help of an automated ground system) can generate an arrival tree (arrival route from each of the TMA entry points to the metering fix) depending on the traffic density and distribution.

Ideally, this should take place as soon as aircraft enter the TMA. However, this is feasible only if the flight sequence is generated while aircraft are still in cruise and before the optimum top of descent (TOD). Then, the FMS on board can compute the neutral trajectory (i.e., idle thrust, no speed brakes usage) that follows the route requested by the ATCO. If this is not possible, the communication between aircraft and ATC should be established before the TMA, e.g., in an hypothetical E-TMA entry point or in the en-route phase, allowing for sufficient time for the required computations. Thus, choosing TMA arrival time from a time window is feasible.

B. Framework Components

Our approach consists of two main steps:

1. Computation of CDO speed profiles for different lengths of the entry-point–runway path for all aircraft in the considered time interval.
2. Computation of the arrival trees, that allow for temporal separation of all considered aircraft flying along the computed arrival paths using CDO speed profiles, for the considered time interval, where the required temporal separation depends on the aircraft categories of the leading and trailing aircraft.

For 2. we use a discretization: we overlay the TMA with a square grid and use directed edges to grid neighbors as possible building blocks of our arrival tree. Hence, any entry-point–runway path has a length from a discrete set (the possible lengths from shortest entry-point–runway grid path to longest edge-disjoint entry-point–runway grid path). For all possible discrete path lengths, for each aircraft, we compute the CDO speed profiles (1.), see Section V for details: for a given route length we optimize the vertical profile, where we assume neutral CDOs for all descents. Our computation of arrival trees (2.) uses a MIP formulation, see Section IV for the MIP construction.

IV. Grid-Based MIP Formulation

In Subsection IV-A, we review our MIP model from [5], in Subsection IV-B, we detail new constraints for flexible entry times and wake-turbulence-category based separation.

A. Review of Our Previous Model

In [5], we presented a MIP formulation for dynamic arrival routes of aircraft following specific speed profiles with guaranteed temporal separation. We required a temporal separation of σ between all consecutive aircraft, i.e., we did not take aircraft of different categories and the resulting separation into account, but used a uniform value. Moreover, the arrival time of all aircraft to the entry point was given as input and fixed.

The MIP formulation is based on a grid. We build an arrival tree that has the runway as its root, and the entry points as leaves. We add several constraints to yield multiple operational requirements:

1) No more than two routes merge at a point. Merge points require more ATCO attention, we aim for lowest possible traffic complexity around merges.
2) Merge points are separated by a minimum distance to impede high traffic complexity focused in a small area.
3) Aircraft dynamics prohibit arbitrarily acute turns.
4) Obstacles (e.g., no-fly zones) are avoided.

The complete MIP resulting from these constraints, the temporal separation of σ (aircraft following the computed entry-point-runway paths along the arrival tree are temporally separated), the CDO speed profiles, and some further constraints is given in [5]: objective function (8) and Constraints (2), (5), (9)-(22), (34)-(42), (44-56).

B. New Constraints

We aim to schedule as many arriving aircraft with a CDO profile as possible, to ensure that, we allow deviation from the planned time at the TMA entry points, see Subsubsection IV-B1. Moreover, in Subsubsection IV-B2, we include separation criteria based on the wake turbulence categories of the leading and trailing aircraft (i.e., we deviate from a uniform σ).

We recapitulate some notation from [5]. For each aircraft a we are given a set of speed profiles $\mathcal{S}(a)$; for γ being an upper bound on the number of grid vertices in any arrival path, we define $\mathcal{L} = \{1, \dots, \gamma\}$; and we consider the time interval $\overline{T} = \{0 \dots, T\}$. The set of entry points to the TMA is denoted as $\mathcal{P}$. We use binary variables $y_{a,j,p,n,t}$ that indicate whether aircraft a using speed profile p occupies the n-th vertex j at time t.

1) Flexibility at TMA Entry Points: When two aircraft arriving consecutively at the same entry point undercut the required temporal separation at the entry point, this yields infeasibility already at the entry point, and they cannot be scheduled. To schedule even such aircraft, instead of requiring that aircraft a arrives at its entry point b at the given time t_a^b, we allow for it to arrive in the time interval $[t_a^{b,1}, t_a^{b,2}]$. For the MIP from [5], this means that we substitute Constraints (34), (35), (36) and (44) by Constraints (1), (2), (3) and (4), and add Constraint (5), which ensures that aircraft a cannot be at any node before $t_a^{b,1}$. Constraint (1) ensures that for each aircraft a and its entry point b, exactly one speed profile p is chosen and the aircraft arrives at exactly one time in $[t_a^{b,1}, t_a^{b,2}]$. Constraints (2), (3) set several of the y-variables to zero, and Constraint (4) ensures that for the speed profile of the correct length (the length $\ell(b)$ of the arrival path from b) the variable y is set to one (with constraints (45)-(48) in [5] we ensure that the binary variable $\psi_{b,a,p}$ is set to 0 iff $p = \ell(b)$).

$$\sum_{t=t_a^{b,1}}^{t_a^{b,2}} \sum_{p \in \mathcal{S}(a)} y_{a,b,p,1,t} = 1 \qquad \forall b \in \mathcal{P}, \forall a \in \mathcal{A}_b \tag{1}$$

$$y_{a,b,p,k,t} = 0 \qquad \forall b \in \mathcal{P}, \forall a \in \mathcal{A}_b, \forall p \in \mathcal{S}(a), \forall t \le t_a^{b,1}, \forall k \ne 1 \in \mathcal{L} \tag{2}$$

$$y_{a,b,p,1,t_a^b} = 0 \qquad \forall b \in \mathcal{P}, \forall a \in \mathcal{A}_b, \forall p \in \mathcal{S}(a), \forall t \in T : t_a^{b,1} < t < t_a^{b,2} \tag{3}$$

$$\sum_{t=t_a^{b,1}}^{t_a^{b,2}} y_{a,b,p,1,t} = 1 - \psi_{b,a,p} \ \forall b \in \mathcal{P}, \forall a \in \mathcal{A}_b, \forall p \in \mathcal{S}(a) \tag{4}$$

$$y_{a,j,p,k,t} = 0 \quad \forall b \in \mathcal{P}, \forall a \in \mathcal{A}_b, \forall p \in \mathcal{S}(a), \forall t < t_a^{b,1}, \forall k \in \mathcal{L} \tag{5}$$

2) Separation with Different Wake Turbulence Categories: We use ICAO's aircraft categories: LIGHT (L), MEDIUM (M), HEAVY (H) (SUPER can easily be included in our concept as well). We define $C_1 = \{\text{H,M}\}$, and $C_2 = \{\text{L}\}$. Let $\sigma_{A,B}$ be the temporal separation if the leading aircraft is of category A and the trailing aircraft is of category B.

Each aircraft a is an element of either set A or B. We choose $\Omega = \max \sigma_{A,B}$. If the leading and trailing aircraft are

of two different ($A \neq B$) or the same category, we enforce a temporal separation of $\sigma_{A,B}$ and $\sigma_{A,A}$ using a constraint of type (6) (for all categories A, B) and a constraint of type (7) (for all categories A), respectively.

$$\sum_{a\in B}\sum_{p\in\mathcal{S}(a)}\sum_{k\in\mathcal{L}}\sum_{\tau=t}^{t+\sigma_{AB}-1} y_{a,j,p,k,\tau} \leq \Omega - \Omega \cdot \sum_{a'\in A}\sum_{\substack{p'\in\\ \mathcal{S}(a')}}\sum_{k'\in\mathcal{L}} y_{a',j,p',k',t}$$
$$\forall j \in V, \forall t \in \{0,\ldots,\overline{T}-\sigma_{A,B}\} \quad (6)$$

$$\sum_{a\neq a'\in A}\sum_{p\in\mathcal{S}(a)}\sum_{k\in\mathcal{L}}\sum_{\tau=t}^{t+\sigma_{AA}-1} y_{a,j,p,k,\tau} \leq \Omega - \Omega \cdot y_{a',j,p',k',t}$$
$$\forall a' \in A, \forall p \in \mathcal{S}(a') \forall j \in V, \forall t \in \{0,\ldots,\overline{T}-\sigma_{A,A}\} \quad (7)$$

V. Generation of CDO Profiles

We compute several descent trajectories for each arriving aircraft for each possible route length within the TMA. We assumed neutral CDOs for all the descents, with no additional thrust (only idle thrust) nor speed-brakes usage allowed.

A. Optimal Control Problem for Aircraft Descents

Given a route length (yielding a fixed distance to go), the optimization of the vertical profile (altitude and speed) can be stated as an optimal control problem: the control time history of a system, here the aircraft, is computed, such that a cost function is minimized while satisfying some dynamic and operational constraints [5]. We consider a point-mass representation of the aircraft reduced to a "gamma-command" model, where vertical equilibrium is assumed (lift balances weight).

The trajectory is divided in two phases: the latter part of the cruise phase prior the TOD, and the idle descent down to the metering fix. Assuming that the original cruise speed will not be modified after the optimization process, the two-phases optimal control problem can be converted into a single-phase optimal control problem [15], [17].

Only one control variable exists in the formulas used to generate the neutral CDOs, which appears linearly in the equations describing the dynamics of the system and in the cost function to be minimized. The resulting singular optimal control problem can be solved semi-analytically from the implicit formulation of optimal singular arcs [17].

B. Speed profiles

We simulate realistic neutral CDO speed profiles for all considered aircraft assuming no wind and international standard atmospheric conditions (ISA). Furthermore, we took into account aircraft model, current altitude and true airspeed at the top of descent, as well as the distance to go (which defines which exact speed profile the aircraft is taking).

An example of a set of speed profiles for two aircraft models is shown in Figure 1. We compute the profiles for several paths inside the TMA for all possible route lengths (leading to different distances to go). The two aircraft models belong to two different ICAO categories: an Embraer EMB-500 Phenom 100 (light) and an Airbus A320 (medium). In addition, same initial cruise altitude and speed were considered for both aircraft. We can observe that for the same distance to go, the airspeed of the light aircraft is lower than that of the medium aircraft, i.e., it takes longer for the light aircraft to fly each of the segments in the TMA.

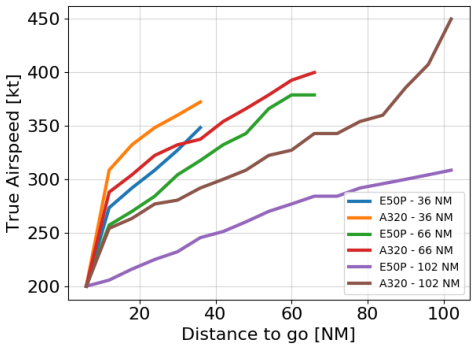

Figure 1. Speed profiles inside the TMA for an E50P and an A320.

VI. Experimental Study

In this section, we apply our framework to a real-world instance of arrivals at Stockholm TMA (Subsec.VI-A). We consider traffic arriving within one hour as input and compute the dynamic arrival routes with guaranteed temporal separation for that hour, where aircraft arrival times might deviate within a predefined interval from the historical aircraft arrival times at TMA entry points, see Subsubsec.VI-A1. In a second experiment, Subsubsec.VI-A2, we alter the fleet mix to show the influence of heterogeneous traffic on the possibility to accommodate CDO speed profiles for all aircraft. In Subsec.VI-A, we describe indata and experimental results, in Subsec.VI-B and VI-C, we analyze the obtained arrival routes w.r.t. different KPIs, distance in TMA and vertical efficiency.

A. Experiments

We have chosen a data sample for one of the busiest hours of operation in 2018: May 16, 2018, 5:00AM-6:00AM. We obtain historical flight trajectories from the open source database of the Opensky Network [18]. Aircraft performance parameters for CDO trajectory generation are input from BADA 4.1 [19]. In case the aircraft model does not correspond to any of the BADA models, a comparable aircraft in terms of performance and dimensions is used.

We solve our MIP using the Gurobi optimization solver installed on a powerful Tetralith server [20], utilizing Intel HNS2600BPB computer nodes with 32 CPU cores, 384 GB, provided by the Swedish National Infrastructure for Computing (SNIC).

We split the considered hour into two periods of 30 minutes. For each half hour, the arrival tree is optimized w.r.t. the traffic in that period. The routes often get stretched for the purpose of conflict resolution. But when the aircraft in potential conflict have passed merge points or already landed, other aircraft

continue flying along sub-optimal routes. Adapting the tree configuration every 20-30 minutes, which is about the average aircraft time in TMA, will keep them optimized for the actual traffic situation. In [5], we presented constraints ((54)-(56)) to enforce consistency between consecutive trees, i.e., no large deviation of the second-period tree from the first-period tree.

We use an 11x15 grid, which automatically yields merge point separation of $\sim$6 NM. In current operations, a separation of 5 NM is used, that is, we show results in the operational separation range (using a finer 14x19 grid, resulting in 5NM separation, makes the problem computationally too expensive).

Based on ICAO's separation minima [21], we define $\sigma_{C_1,C_2} = 3$ mins, $\sigma_{C_1,C_1} = \sigma_{C_2,C_2} = \sigma_{C_2,C_1} = 2$ mins.

Finally, for any given flight, the number of trajectories generated corresponds to the number of possible routes the aircraft can fly. In this case, we considered path lengths within the TMA from 30 NM (corresponding to the minimum path length within the grid) to 108 NM, with each path split into several segments of constant length of 6 NM. For instance, a 30 NM path inside the TMA would be split into 5 segments. In total, we compute 14 trajectories per flight (i.e., 14 possible path lengths ranging from 30 NM to 108NM). In addition, we generated all those trajectories such that we ensure the same time at the TMA entry point, to that end we use different cost index values for each trajectory. We chose the distance in this experiment according to the grid size. The lower bound stems directly from the grid; additionally, we impose a large enough upper bound to allow for feasible solutions.

1) Experiment 1. Original Traffic from May 16, 2018, 5:00 AM-6:00AM: In the first experiment, we use the original traffic data from May 16, 2018, 5:00 AM-6:00AM: 30 aircraft according to Opensky network data. We use $t_a^{b,1} = t_a^b - 5$ mins, $t_a^{b,2} = t_a^b + 5$ mins, that is, all aircraft are scheduled to arrive at the entry point within ± 5 minutes around the original arrival time on May 16, 2018. In a real situation, this change in the entry time could be achieved during the en-route phase. In previous work these modifications in entry time were shown to be feasible; for typical cost indexes between 30 kg/min and 100 kg/min, aircraft can gain/lose between 1.2 seconds/NM and 4 seconds/NM [22]. Hence, by assuming a cruise length of 75 NM to 250 NM, aircraft would be able to arrive within $\pm$ 5 minutes to the TMA entry point. These values depend on several factors, like the aircraft type or the cruise flight level. Also the wind can affect the time that can be gained/lost during cruise [23]. In these situations, the communication (or trajectory synchronisation) between the aircraft and the ATCO should be established way before entering the TMA, so that the aircraft can lose or gain the requested time during cruise.

Figure 2(a) shows the resulting arrival route trees for the two half hours within the 1-hour period. Table I gives the resulting schedule, all (merge) points used are marked in Figure 2(a). In fact, we present a solution for the interval 4:51–6:02 AM, as the first aircraft landing between 5 and 6 AM arrives to the TMA at 4:51, and the last aircraft (due to our possible shift of 5 minutes) lands at 6:02 AM. The average entry time deviation—the absolute value of the difference between the original time of aircraft arrival to TMA and the scheduled entry time according to our optimized arrival schedule—is 2.27 minutes. The total length of all routes is 216 NM for the first tree and 198 NM for the second tree. Figure 3 illustrates the arriving schedule at all merge points and on the runway. The average time separation at the runway is 2.14 min.

TABLE I. OPTIMIZED TIME SCHEDULE FOR 30 ARRIVING AIRCRAFT WITHIN STOCKHOLM ARLANDA TMA BETWEEN 4:50 AND 6:02 AM ON MAY 16, 2018.

Aircraft	Entry point	Entry	M1	M2	M3	M4	rwy
a1	Ent1 (West)	4:51	-	4:53	-	4:57	4:59
a2	Ent2 (South)	4:52	4:58	-	-	4:59	5:01
a3	Ent3 (North)	4:51	-	4:57	-	5:01	5:03
a4	Ent2	4:56	5:02	-	-	5:03	5:05
a5	Ent3	4:55	-	5:01	-	5:05	5:07
a6	Ent3	4:58	-	5:04	-	5:08	5:09
a7	Ent1	5:04	-	5:06	-	5:10	5:11
a8	Ent1	5:06	-	5:08	-	5:12	5:14
a9	Ent4 (East)	5:06	5:14	-	-	5:15	5:16
a10	Ent3	5:07	-	5:13	-	5:17	5:18
a11	Ent3	5:09	-	5:15	-	5:19	5:20
a12	Ent3	5:11	-	5:17	-	5:21	5:23
a13	Ent2	5:09	5:21	-	-	5:23	5:25
a14	Ent4	5:17	5:25	-	-	5:26	5:27
a15	Ent3	5:18	-	5:24	-	5:28	5:29
a16	Ent4	5:24	-	-	5:29	5:30	5:31
a17	Ent2	5:25	-	-	5:31	5:32	5:33
a18	Ent2	5:27	-	-	5:33	5:34	5:35
a19	Ent2	5:29	-	-	5:35	5:36	5:37
a20	Ent4	5:32	-	-	5:37	5:38	5:39
a21	Ent3	5:30	-	5:36	-	5:40	5:41
a22	Ent1	5:36	-	5:38	-	5:42	5:43
a23	Ent1	5:38	-	5:40	-	5:44	5:45
a24	Ent4	5:40	-	-	5:45	5:46	5:47
a25	Ent4	5:42	-	-	5:47	5:48	5:49
a26	Ent4	5:44	-	-	5:49	5:50	5:51
a27	Ent1	5:46	-	5:48	-	5:52	5:53
a28	Ent3	5:44	-	5:50	-	5:55	5:57
a29	Ent3	5:48	-	5:54	-	5:58	5:59
a30	Ent2	5:54	-	-	6:00	6:01	6:02

2) Experiment 2. Changed Fleet Mix—More Light Aircraft: In this experiment, we aim to highlight the influence of the presence of different aircraft categories in the mix. To this end, we increase the share of light aircraft in the fleet mix to 20%: we replace six randomly chosen aircraft from the first experiment with light aircraft types, more specifically an Embraer EMB-500 Phenom 100. Note that this is unrealistic for Arlanda, the share is usually much lower, and the majority of aircraft are of the medium category. In 2018, light aircraft did not constitute more than 1% of the total traffic [24]. We choose this artificial fleet mix for a proof of concept experiment. Light aircraft typically have slower speed profiles for arrivals (see Figure 1), hence, this limits the throughput. Moreover, because of wake vortices, a trailing light aircraft (as opposed to a trailing aircraft of another category) requires larger separation to a leading heavier aircraft.

Thus, only 25 out of 30 aircraft could be scheduled—again using a possible time window of ± 5 minutes around the original arrival time. Figure 2(a) illustrates the resulting arrival route trees for the two half hours within the 1-hour period (we yield the same trees as in Experiment 1). The average entry time deviation is 2.03 minutes. The resulting schedule is shown

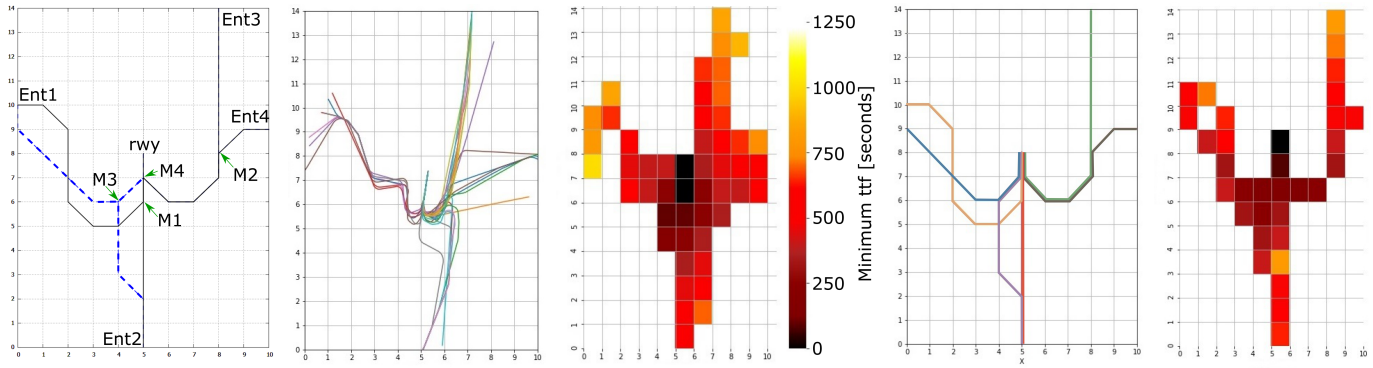

Figure 2. (a): Arrival route trees calculated using the optimization framework for 30 aircraft present in Arlanda TMA between 5:00 AM and 6:00 AM on May 16, 2018, which arrive during the two periods: 4:50-5:30 AM (shown in black), 5:30-6:02 AM (shown in blue dashed). Entry points and merge points are reference points for the time schedules presented in Table I and Table II. (b)-(e): Real arrival routes vs. optimized arrival routes on May 16, from 4:50 to 6:02 AM: routes in (b)/(d), minimum ttf in (c)/(e). The scale shown in (c) is valid also for (e).

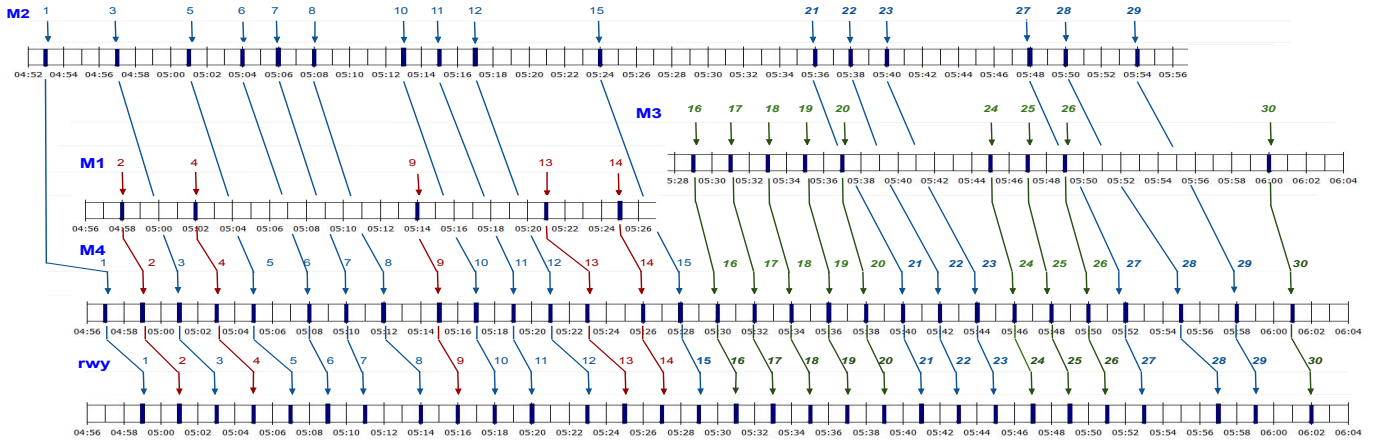

Figure 3. Experiment 1: arrival time schedule at all merge points of the optimized arrival trees for 30 aircraft within Stockholm Arlanda TMA between 4:50 and 6 am on May 16, 2018. Bold italic numbers refer to arrivals on the tree for the second half hour.

in Table II and Figure 4 illustrates the runway arrival schedule.

B. Evaluation of Arrival Sequencing

Our optimized solutions guarantee separation with the chosen separation parameter $\sigma_{A,B}$. We evaluate the benefits provided by this approach using a set of KPIs recently proposed by Eurocontrol EEC in [14], with several adjustments to the proposed methodology, which are detailed in [25]. All evaluations in Subsections VI-B and VI-C are done for Experiment 1.

1) Minimum Time to Final: The **time to final** (ttf) is defined as the time from an aircraft's current position to the final approach point. We calculate the **minimum time to final** as the minimum time needed from any point within a grid cell to the final approach along any of the aircraft trajectories passing through the cell. Figure 2(b)/(c) and (d)/(e) show the routes and the time to final for the original traffic from May 16, 2018, 5:00 AM-6:00AM and for the optimized routes, respectively. For the real-world trajectories, the minimum time to final lies between 0 and 986, with an average of 494 seconds (SD=228); for the optimized trajectories, the minimum time to final lies between 0 and 660, with an average of 331 seconds (SD=161).

2) Spacing Deviation: The **spacing** of an arriving aircraft pair at time t is defined as the difference between the respective times to final. The **spacing deviation** (sd) is computed for pairs of leading and trailing aircraft at time t; it captures the aircraft's mutual position in time. It is calculated using Equation (8):

$$\text{sd}(t) = \min\ \text{ttf}(\text{trailer}(t)) - \min\ \text{ttf}(\text{leader}(t - s_{rwy})) \quad (8)$$

where s_{rwy} is the temporal separation at the runway.

The spacing deviation reflects information about the control error, which is the accuracy of spacing around the airport. Figure 5(a) and (b) show the spacing deviation for the original traffic from May 16, 2018, 5:00 AM-6:00AM and for the optimized routes, respectively. For the real-world and optimized trajectories the spacing deviation lies between -328 and 338, and -300 and 300 with an average of -2.86 (SD=86.25) and 16.42 (SD=69.45), respectively. The maximum width of the 90th quantile (shown in turquoise in Figure 5(a) and (b)) is

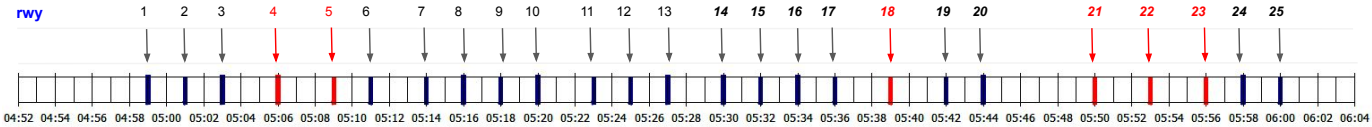

Figure 4. Experiment 2: optimized arrival time schedule at the runway for 25 arriving aircraft with about 20% of light aircraft randomly added to the original fleet mix within Stockholm Arlanda TMA between 4:50 and 6 am on May 16, 2018. Light aircraft are shown in red, bold italic numbers refer to arrivals on the tree for the second half hour.

TABLE II. OPTIMIZED TIME SCHEDULE FOR 25 ARRIVING AIRCRAFT WITH ABOUT 20% OF LIGHT AIRCRAFT RANDOMLY ADDED TO THE ORIGINAL FLEET MIX (COLORED IN RED) WITHIN STOCKHOLM ARLANDA TMA BETWEEN 4:50 AND 6:00 AM ON MAY 16, 2018.

Aircraft	Entry point	Entry	M1	M2	M3	M4	rwy
a1	Ent1 (West)	4:51	-	4:53	-	4:57	4:59
a2	Ent2 (South)	4:52	4:58	-	-	4:59	5:01
a3	Ent3 (North)	4:51	-	4:57	-	5:01	5:03
a4	Ent3	4:54	-	5:00	-	5:04	5:06
a5	Ent3	4:57	-	5:03	-	5:07	5:09
a6	Ent1	5:04	-	5:06	-	5:10	5:11
a7	Ent1	5:06	-	5:08	-	5:12	5:14
a8	Ent4 (East)	5:06	5:14	-	-	5:15	5:16
a9	Ent3	5:07	-	5:13	-	5:17	5:18
a10	Ent3	5:09	-	5:15	-	5:19	5:20
a11	Ent3	5:11	-	5:17	-	5:21	5:23
a12	Ent2	5:09	5:21	-	-	5:23	5:25
a13	Ent4	5:17	5:25	-	-	5:26	5:27
a14	Ent4	5:23	-	-	5:28	5:29	5:30
a15	Ent2	5:24	-	-	5:30	5:31	5:32
a16	Ent2	5:26	-	-	5:32	5:33	5:34
a17	Ent4	5:29	-	-	5:34	5:35	5:36
a18	Ent4	5:32	-	-	5:37	5:38	5:39
a19	Ent2	5:34	-	-	5:40	5:41	5:42
a20	Ent1	5:37	-	5:39	-	5:43	5:44
a21	Ent3	5:37	-	5:43	-	5:48	5:50
a22	Ent2	5:44	-	-	5:50	5:51	5:53
a23	Ent1	5:48	-	5:50	-	5:54	5:56
a24	Ent3	5:47	-	5:53	-	5:57	5:58
a25	Ent4	5:53	-	-	5:58	5:59	6:00

427 and 537 for the real-world and the optimized trajectories, respectively.

3) Sequence Pressure: The **sequence pressure** for an aircraft at time t is the number of aircraft with the same time to final within a given time window; it reflects the aircraft density. It is calculated for each aircraft at any time of its presence within the TMA with the discrete time steps.

We choose a window of 2 minutes (the minimum separation requirement in our optimization framework). Figure 5(c) and (d) show the sequence pressure for the original traffic from May 16, 2018, 5:00 AM-6:00AM and for the optimized routes, respectively. For the real-world and optimized trajectories the sequence pressure at 120 seconds lies between 4 and 1 and is 1 with an average of 1.38 (SD=0.65) and 1 (SD=0), respectively.

4) Analysis: Comparing Figure 2(c) and (e), we observe a reduction in lateral dispersion in the optimized solution since all aircraft follow the same predefined routes. Moreover, our solution provides significant reduction in average time aircraft spend in TMA (9.5 min vs. 15.1 min for real flights). We also observe a substantial reduction of the sequence pressure from original traffic to optimized routes. While the spacing deviation is not considerably reduced, an implementation of the proposed fully automated separation is expected to reduce ATCO workload, as he/she will not be responsible for providing safe separation via vectoring, but rather observe the predefined aircraft progress and apply minor corrections only in case of unexpected situations.

C. Vertical Efficiency and Distance Flown in TMA

An analysis of the vertical efficiency reveals significant differences between the actual flown trajectories and the corresponding flights performing neutral CDOs. Figure 6 illustrates the two trajectory types and clearly demonstrates that actual flown profiles (orange) reach a lower altitude earlier than neutral CDOs (blue), which stay a longer time in cruise before starting the descent. Furthermore, actual trajectories contain long periods of level flight (some of them at very low altitudes), which unavoidably results in extra fuel burn and high levels of noise.

Even a comparison of the distance flown inside the TMA shows a clear difference between the actual flights and the corresponding optimized trajectories, see Figure 7. Note that the values for the optimized routes are an approximation: we count all tree edges with 6NM, though in fact the axis-parallel edges are shorter and the diagonal edges are longer. The total distance covered by all 30 aircraft is 1958 NM and 1578 NM for the actual and the optimized trajectories, respectively.

VII. CONCLUSION

In this work, we show that enabling flexible entry times allows that all aircraft arriving at Stockholm Arlanda during one of the busiest hours of operation can fly CDOs on arrival routes that guarantee temporal separation of all aircraft—this takes separation requirements based on the different aircraft categories in the fleet mix into account. Hence, our solution contributes both to reduced environmental impact and automation ground support for ATCOs. We show that our optimized routes provide improvements in vertical efficiency, distance and average time in TMA.

In order to ensure aircraft will be able to arrive at the TMA at a time that differs from their planned time of arrival, the communication between the flight crew and the ATCOs should be established before the TMA entry point. We propose a concept of operations where ATCOs contact the aircraft in an hypothetical E-TMA entry point or, depending on the traffic complexity, even in the en-route phase. Thus, aircraft will be able to gain/lose this amount of time by modifying their flight profiles accordingly.

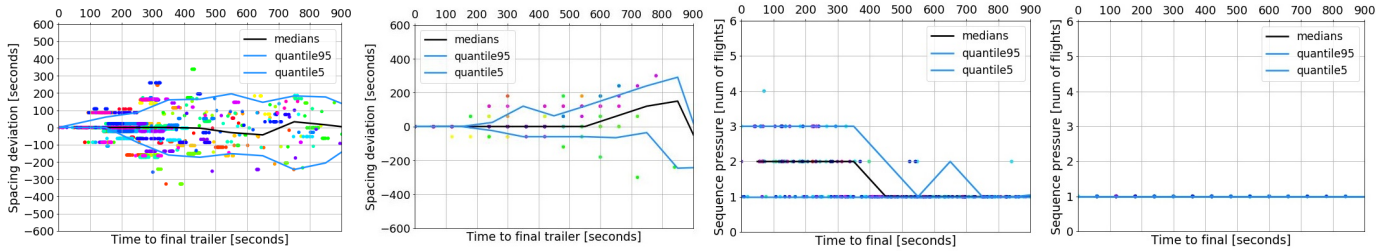

(a) (b) (c) (d)

Figure 5. Spacing deviation and sequence pressure for the real arrival routes vs. optimized on May 16, from 4:50 to 6:05 AM.

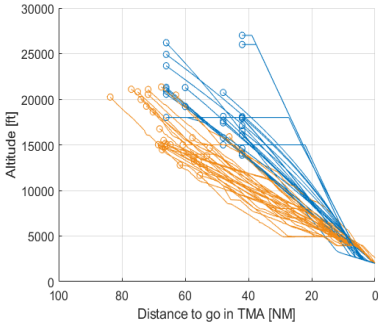

Figure 6. Comparison of the vertical profiles of the actual (orange) vs. optimized CDO-enabled routes (blue) for 30 arrivals within Stockholm Arlanda TMA between 4:50 and 6:02 AM on May 16, 2018.

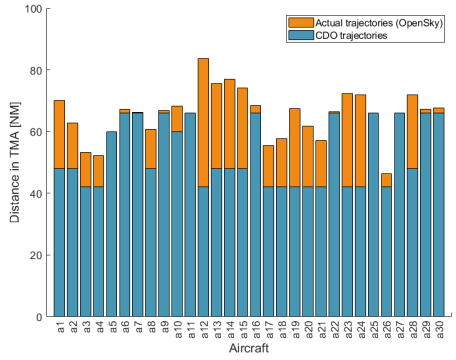

Figure 7. Comparison of the distance flown in the TMA of the actual (orange) vs. optimized CDO-enabled routes (blue) for 30 arrivals within Stockholm TMA on May 16, 2018.

In future work, we aim to also evaluate the noise impact and lateral efficiency. Moreover, we plan to analyze a possible trade-off between robustness and uncertainty.

REFERENCES

[1] "IATA air passenger forecast shows dip in long-term demand," https://www.iata.org/en/pressroom/pr/2015-11-26-01/, acc. Oct 08, 2020.

[2] S. M. Iacus, F. Natale, C. Santamaria, S. Spyratos, and M. Vespe, "Estimating and projecting air passenger traffic during the COVID-19 coronavirus outbreak and its socio-economic impact," *Safety Science*, vol. 129, p. 104791, 2020.

[3] ICAO, "Continuous descent operations (CDO) manual-doc 9931/an/476," ICAO, Tech. Rep., 2010, montreal, Quebec, Canada.

[4] Eurocontrol, "Continuous climb and descent operations," https://www.eurocontrol.int/concept/continuous-climb-and-descent-operations, 2019, accessed Oct 08, 2020.

[5] R. Sáez, X. Prats, T. Polishchuk, V. Polishchuk, and C. Schmidt, "Automation for Separation with CDOs: Dynamic Aircraft Arrival Routes," *AIAA J of Air Transp.*, vol. 28, no. 4, pp. 144–154, 2020.

[6] Y. Xu and X. Prats, "Effects of linear holding for reducing additional flight delays without extra fuel consumption," *Transportation Research Part D: Transport and Environment*, vol. 53, no. 1, pp. 388–397, 2017.

[7] "NATS and Eurocontrol, operational service and environment definition (OSED) for time based separation for arrivals (TBS)."

[8] D. Ivanescu, C. Shaw, E. Hoffman, and K. Zeghal, *Towards Performance Requirements for Airborne Spacing- A Sensitivity Analysis of Spacing Accuracy*.

[9] H. Balakrishnan and B. Chandran, *Scheduling Aircraft Landings Under Constrained Position Shifting*, 2012.

[10] L. Credeur, W. R. Capron, G. W. Lohr, D. J. Crawford, T. D. A, and W. G. J. Rodgers, "Final approach spacing aids (FASA) evaluation for terminal area, time-based air traffic control," 1993, Hampton, VA: NASA-TP-3399.

[11] T. Callantine, P. Lee, J. Mercer, T. Prev, and E. Palmer, "Air and ground simulation of terminal-area FMS arrivals with airborne spacing and merging," in *6th ATM Seminar*, 2005.

[12] J. E. Robinson III, J. Thipphavong, and W. C. Johnson, "Enabling performance-based navigation arrivals: Development and simulation testing of the terminal sequencing and spacing system," in *11th ATM Seminar*, 2015.

[13] R. Christien, A. Trzmiel, and K. Zeghal, "Toward the characterisation of sequencing arrivals," in *12th ATM Seminar*, 2017.

[14] R. Christien, E. Hoffman, and K. Zeghal, "Spacing and pressure to characterise arrival sequencing," in *13th ATM Seminar*, 2019.

[15] R. Sáez, R. Dalmau, and X. Prats, "Optimal assignment of 4D close-loop instructions to enable CDOs in dense TMAs," in *IEEE/AIAA 37th DASC*, London, England, UK, 2018.

[16] A. Lemetti, T. Polishchuk, V. Polishchuk, R. Sáez, and X. Prats, "Identification of Significant Impact Factors on Arrival Flight Efficiency within TMA," in *9th ICRAT*, 2020.

[17] S. G. Park, P. Dutta, and P. K. Menon, "Optimal Trajectory Option Sets for In-Flight Climb-Descend Trajectory Negotiations," in *17th AIAA ATIO*, Denver, CO, June 2017.

[18] "OpenSky Network," https://opensky-network.org, July 2019, accessed on December 2, 2018.

[19] Eurocontrol, "User Manual for the Base of Aircraft Data (BADA) Family 4," 2014.

[20] "Tetralith server, NSC, Linköping University," https://www.nsc.liu.se/systems/tetralith/, 2019, accessed on 28/01/2019.

[21] SKYbrary, "Mitigation of wake turbulence hazard, wake turbulence separation minima," https://www.skybrary.aero/index.php/Mitigation_of_Wake_Turbulence_Hazard, acc. Sept 26, 2020.

[22] L. Delgado and X. Prats, "En Route Speed Reduction Concept for Absorbing Air Traffic Flow Management Delays," *Journal of Aircraft*, vol. 49, no. 1, pp. 214–224, 2012.

[23] L. Delgado and X. Prats, "Effect of wind on operating-cost-based cruise speed reduction for delay absorption," *IEEE Trans Intell Transp Syst*, vol. 14, no. 2, pp. 918–927, 2013.

[24] L. Smetanová, A. Ulanovský, and P. Hluska, "Analysis of the Typical Fleet Mix for Stockholm Arlanda Airport Arrivals," 2019. [Online]. Available: http://weber.itn.liu.se/~tatpo46/pps/Q3_final_fleetmix.pdf

[25] L. Smetanová, "Evaluation of arrival sequencing at arlanda airport," M.S. thesis, Linköping University and Czech Techical University, 2020.